

Static spherically symmetric solutions of the $f(R)$ gravity

V. I. Zhdanov^{1,*}

¹*Taras Shevchenko National University of Kyiv, Kyiv 01601, Ukraine*

(Dated: December 2024)

Static spherically symmetric (SSS) solutions of $f(R)$ gravity are studied in the Einstein frame. The solutions involve SSS configuration mass M and scalaron mass μ (in geometrized units). For typical astrophysical masses, the dimensionless parameter $M\mu$ has very large value. We found analytic solutions on a finite interval for $M\mu \rightarrow \infty$ in case of a family of scalaron potentials. The asymptotically flat solutions on $(0, \infty)$ have been studied numerically for $M\mu$ up to 10^{20} in case of the quadratic $f(R)$ model.

Keywords: spherical symmetry, modified gravity, scalar fields

I. INTRODUCTION

In the $f(R)$ gravity, the gravitational Einstein-Hilbert Lagrangian density is replaced by a more general function of the scalar curvature R (see [1–3] for a review). This leads to fourth-order equations with respect to the space-time metric $g_{\mu\nu}$ (Jordan frame). However, in a number of the $f(R)$ versions, it is possible to reduce the problem to usual Einstein equations with respect to new metric $\hat{g}_{\mu\nu}$ (Einstein frame) by means of conformal transformation [1–3]

$$\hat{g}_{\mu\nu} = e^{2\xi} g_{\mu\nu}, \quad (1)$$

where some scalar field ξ dubbed scalaron¹ satisfies an additional nonlinear wave equation that involves a scalaron mass μ .

Natural questions arise concerning the possible role of the $f(R)$ gravity in compact astrophysical objects. Most publications on this subject deal with the black-hole configurations [5–9]. The static spherically symmetric (SSS) objects without a horizon have been investigated in [4, 10]. Such objects turn out to be either linearly stable or unstable depending on the choice of configuration parameters [4].

In different $f(R)$ theories, the scalaron masses vary from $\sim 10^{13}$ GeV to ~ 4 meV (see, e.g., [11, 12]). This yields very large dimensionless $M\mu$ (in geometrized units²), where M is the configuration mass. The latter, comparatively small, value of μ corresponds to length scale $l_\mu \sim 5 \cdot 10^{-3}$ cm yielding for the Solar mass $\mu M = M/l_\mu \simeq 3 \cdot 10^9$ and another 8-9 orders of magnitude more for typical masses of the central objects in active galactic nuclei. This leads to exponentially large

numbers and creates some difficulties for application of standard numerical algorithms to investigation of SSS configurations. Note that the numerical results obtained in [4, 10] in a case of the quadratic $f(R)$ model deal only with modest $M\mu$.

In this paper, we consider approximate SSS solutions for sufficiently large $M\mu$. For numerical estimates we use the scalaron potential of the quadratic $f(R)$ gravity [11], see also [10, 12].

This paper is organized as follows. In Section II, we review the relations of $f(R)$ gravity in the Einstein frame for SSS configurations. The basic equations in a suitable form for consideration of large $M\mu$ are presented in Section III. Then we justify the approximate solutions for a special class of the scalaron potentials IV. In Section V we perform numerical calculations to illustrate the solutions. In Section VI, we discuss our results.

II. BASIC EQUATIONS IN THE EINSTEIN FRAME

The well known example when the transition to the Einstein frame is possible by means of transformation (1) is due to the quadratic $f(R)$ [11–13]; the corresponding scalaron self-interaction potential $W(\xi)$ is [11–13];

$$W(\xi) = \mu^2 w(\xi), \quad w(\xi) = \frac{3}{4} (1 - e^{-2\xi})^2. \quad (2)$$

For the SSS space-time we use the Schwarzschild (curvature) coordinates

$$d\hat{s}^2 \equiv \hat{g}_{\mu\nu} dx^\mu dx^\nu = e^\alpha dt^2 - e^\beta dr^2 - r^2 dO^2, \quad (3)$$

where $r > 0$, $\alpha \equiv \alpha(r)$, $\beta \equiv \beta(r)$ and $dO^2 = d\theta^2 + \sin^2 \theta d\varphi^2$ stands for the metric element on the unit sphere.

In absence of non-gravitational fields, the nontrivial equations for static metric (3) in the Einstein frame are (see, e.g., [4])

$$\frac{d}{dr}(\alpha + \beta) = 6r \left(\frac{d\xi}{dr} \right)^2, \quad (4)$$

$$\frac{d}{dr}(\alpha - \beta) = -\frac{2}{r} + \frac{2e^\beta}{r} [1 - r^2 W(\xi)]. \quad (5)$$

* valery.zhdanov@knu.ua

¹ In fact, the canonical scalaron is obtained by some rescaling ξ .

However, following [4], we prefer to use the dimensionless ξ . This explains multipliers in the scalaron potential below.

² $c = \hbar = 8\pi G = 1$; the metric signature is (+ - - -)

where $\xi \equiv \xi(r)$. Equations (4), (5) for α and β must be supplemented by an equation for scalaron ξ :

$$\frac{d}{dr} \left[r^2 e^{\frac{\alpha-\beta}{2}} \frac{d\xi}{dr} \right] = \frac{r^2}{6} e^{\frac{\alpha+\beta}{2}} W'(\xi). \quad (6)$$

In the asymptotically flat static space-time, it is assumed that for $r \rightarrow \infty$ we have $\xi(r) \rightarrow 0$ and Eq. (6) can be approximated by the equation for the linear massive scalar field on the Schwarzschild background

$$\exp[\alpha(r)] = 1 - r_g/r, \quad \exp[\beta(r)] = (1 - r_g/r)^{-1}, \quad (7)$$

where $r_g = 2M$, where $M > 0$ is the configuration mass. Formulas (7) are valid for $r \rightarrow \infty$, since $\xi \rightarrow 0$ tends to zero fairly quickly. However, this is not enough to determine the unique solution of the system (4),(5),(6) and additional information about $\xi(r)$ is needed. For large r , small $\xi(r)$ must decay exponentially with the asymptotic behavior [14–16]

$$\xi(r) = Q \left(\frac{r_g}{r} \right)^{1+M\mu} e^{-\mu r}. \quad (8)$$

The constant Q , which characterizes the strength of the scalar field at infinity, will be called the “scalar charge”. For given M and Q , the asymptotic formulas (7),(8) determine the solution in a unique way [4].

In what follows we will restrict ourselves to positive ξ , where potential (2) has a plateau-like form; this form is preferable for physical reasons in view of cosmological data (see, e.g. [17]).

III. REDUCTION OF EQUATIONS

From rigorous analytical considerations in case of a monotonous function $w(\xi)$, $\xi > 0$ [4] (cf. also a case of a minimally coupled scalar field [18]), it follows that in any non-trivial case there must be some “scalarization region”, where one can hope to see a smoking gun of the modified gravity. In case of the non-monotonous potentials (e.g., the hill-top potentials) numerical simulations show similar behavior at least for sufficiently large $M\mu$. We will focus on the astrophysically interesting case, when the size of this region is large enough, say $\sim (100 \div 1000)r_g$. On the other hand, there must be an interval of small exponentially decaying $\xi(r)$ for $r \geq r_0$; the metric in this region quickly takes on the Schwarzschild values (7) as r grows. This will be labeled as interval A. We assume that r_0 marks a boundary between these two regions and $\xi_0 \equiv \xi(r_0)$ is sufficiently small so as to use formulas (7), (A6), (A6) for $r \geq r_0$. For given $\xi(r_0)$, the value of r_0 can be related with the scalar charge according to (A6).

It may be difficult to perform direct numerical integration of the basic equations in the form (4),(5),(6) for $M\mu \gg 10^{12}$ with a standard software because of exponentially large numbers involved. In order to consider

the problem for large $M\mu$, we introduce new independent variable p by means of the relations

$$r\mu = X_0 + \frac{p}{X_0} \equiv X_0 U(p), \quad U(p) = 1 + \frac{p}{X_0^2}, \quad (9)$$

where $X_0 = \mu r_0 \gg 1$ and the interval $r \in (0, r_0]$ corresponds to negative $p \in (-X_0^2, 0]$. We will move from $p = 0$ to negative values.

Denote

$$\chi = \frac{\alpha + \beta}{2}, \quad Y = U \exp\left(\frac{\alpha - \beta}{2}\right) \quad (10)$$

Equation (4) yields

$$\frac{d\chi}{dp} = 3U \left(\frac{d\xi}{dp} \right)^2, \quad (11)$$

Equation (5) multiplied by $\exp[(\alpha - \beta)/2]$ can be transformed to

$$\frac{dY}{dp} = e^\chi \left[\frac{1}{X_0^2} - U^2 w(\xi) \right]. \quad (12)$$

In terms of (9) and (10), from equation (6) we get

$$\frac{d}{dp} \left[UY \frac{d\xi}{dp} \right] = \frac{U^2}{6X_0^2} e^\chi w'(\xi). \quad (13)$$

By denoting

$$Z = -X_0 UY \frac{d\xi}{dp}, \quad (14)$$

we obtain from (13) two first-order equations

$$\frac{d\xi}{dp} = -\frac{Z}{X_0 UY}, \quad (15)$$

$$\frac{dZ}{dp} = -\frac{U^2}{6X_0} e^\chi w'(\xi). \quad (16)$$

Substitution of (15) into (11) yields

$$\frac{d\chi}{dp} = \frac{3Z^2}{UY^2}. \quad (17)$$

Now we have a closed system of four equations (12),(15),(16),(17) in a normal form, which is ready for the backwards numerical integration³, starting from $p = 0$. Correspondingly, we set initial data at $p = 0$, which corresponds to $r = r_0 > r_g$:

$$\begin{aligned} \xi(0) = \xi_0, \quad Y(0) \equiv Y_0 = \exp\left[\frac{\alpha_0 - \beta_0}{2}\right], \\ \chi(0) = \chi_0, \quad Z_0 = -X_0 Y_0 \left(\frac{d\xi}{dp} \right)_0 \end{aligned} \quad (18)$$

³ The backwards integration is preferable here to, e.g., the shooting method.

From (A5) we get

$$Z_0 = -X_0 Y_0 \left(\frac{d\xi}{dp} \right)_0 = \xi_0 \exp(\alpha_0/2), \quad (19)$$

where $\alpha_0 = \alpha(0)$.

IV. APPROXIMATE SOLUTION

The aim of this Section is to present a family of approximate analytic solutions of (12),(15),(16),(17) in some interval $r \in (0, r_0]$, $r_0 \gg r_g$, which can be useful to check numerical methods.

We consider a class of potentials (2), where⁴

$$w(\xi) = 3\xi^2(1 + O(\xi)), \quad w'(\xi) = 6\xi(1 + O(\xi)) \quad (20)$$

for $|\xi| \ll 1$; also

$$|w(\xi)| \leq w_0 < \infty, \quad |w'(\xi)| \leq w_1 < \infty, \quad (21)$$

and

$$\gamma(\xi) = 1 - \frac{w(\xi)}{3\xi^2} > 0, \quad \xi > 0, \quad (22)$$

where w_0, w_1 and $\gamma(\xi) = O(\xi)$ do not depend on μ . These properties are fulfilled in case of the quadratic $f(R)$ gravity [11, 13], however, the scope of application of the results following from these conditions is much wider; with some caveats it covers, e.g., the case of the hill-top and table-top potentials listed in [17].

The initial conditions for the scalaron field and metric will be imposed at r_0 corresponding to (7), (A6). We fix r_0 and $\xi_0 : 0 < \xi_0 \ll 1$ and consider limit $M\mu \rightarrow \infty$. In this Section we do not discuss the condition of the asymptotic flatness and corresponding solutions for $r \geq r_0$, which may impose additional restrictions on ξ_0 .

Consider the transition region B, where

$$\xi(p) \approx \xi_0, \quad Z(p) \approx Z_0, \quad U(p) \approx 1. \quad (23)$$

We will see that to satisfy these relations it is sufficient to restrict p as follows: $0 > p > p_1 \simeq -\sqrt{X_0}$.

For sufficiently large $M\mu$, the X_0^{-2} term in the right-hand side of (12) can be neglected and equations (12),(17) yield

$$\frac{d\chi}{dp} = \frac{3Z^2}{Y^2}, \quad \frac{dY}{dp} = -e^X w(\xi). \quad (24)$$

Combining these equations, we have

$$\frac{1}{Y^2} \frac{dY}{dp} = -\frac{w(\xi_0)}{3Z_0^2} e^X \frac{d\chi}{dp},$$

whence

$$\frac{1}{Y(p)} = \frac{1}{Y_0} + \frac{w(\xi_0)}{3Z_0^2} [e^{\chi(p)} - e^{\chi_0}]. \quad (25)$$

In view of (19) and (22)

$$e^{\chi_0} \frac{Y_0}{Z_0^2} = \frac{1}{\xi_0^2}, \quad 1 - \frac{Y_0 w(\xi_0)}{3Z_0^2} e^{\chi_0} = \gamma(\xi_0) > 0$$

Then

$$\frac{Y_0}{Y} \approx \frac{1}{Y_*} + e^{X - X_0}, \quad Y_* = \frac{1}{\gamma(\xi_0)}. \quad (26)$$

Now let us assume that for $r = r_0$ the metric takes on the Schwarzschild values, so $\chi_0 = 0$, $|\beta_0| \ll 1$. Using (26) and $Z \approx Z_0$ from (19), equation (17) can be integrated to obtain

$$\begin{aligned} \ln \left(\frac{\gamma(\xi_0) + e^X}{\gamma(\xi_0) + 1} \right) - X - \frac{\gamma(\xi_0)(1 - e^X)}{[\gamma(\xi_0) + e^X][\gamma(\xi_0) + 1]} \\ = -\frac{3\gamma^2(\xi_0)}{Y_0} \xi_0^2 X_0^2 \ln \left(\frac{r}{r_0} \right) \end{aligned} \quad (27)$$

where we take account of $\chi(0) = 0$. From this we have inequality for $-\sqrt{X_0} \leq p \leq 0$

$$\chi(p) \lesssim -3 \frac{\gamma^2(\xi_0)}{Y_0} \xi_0^2 |p|. \quad (28)$$

Using (28) and (21), for $-\sqrt{X_0} \leq p \leq 0$ we get from (16), because of the factor X_0^{-1} in the right-hand side of this equation,

$$|Z(z) - Z_0| \leq \frac{C_1(\xi_0)}{X_0}, \quad |p| \leq \sqrt{X_0}, \quad (29)$$

and using (26), from (15)

$$|\xi(p) - \xi_0| \approx \frac{Z_0}{X_0} (\gamma(\xi_0) + e^X) \leq \frac{C_2(\xi_0)}{\sqrt{X_0}}, \quad (30)$$

where $-\sqrt{X_0} \leq p \leq 0$ and constants $C_1(\xi_0), C_2(\xi_0)$ do not depend on X_0 . These are rough estimates, but they are sufficient for further consideration in case of $X_0 \rightarrow \infty$ and fixed ξ_0 to justify approximations (23) in the region (B).

Owing to (28), for $p_1 = -\sqrt{X_0}$, fixed ξ_0 and large enough $M\mu$

$$\exp[\chi(p_1)] < \exp(-3\gamma^2(\xi_0)Y_0\xi_0^2\sqrt{X_0}) \ll \gamma(\xi_0); \quad (31)$$

this means that $Y(p)$ practically reaches maximal value Y_* in the interval B.

Now we can consider interval C, where $p < p_1$ and we can deal with the exact equations (12) and (16). In consequence of (17) function $\chi(p)$ is monotonous, therefore $\exp \chi(p) < \exp \chi(p_1)$ is bounded by very small constant

$$e^{\chi(p)} < \exp \left(-3 \frac{\gamma^2(\xi_0)}{Y_0} \xi_0^2 \sqrt{X_0} \right) \quad (32)$$

⁴ here the factors 3 and 6 ensure that μ is the scalaron mass corresponding to ξ defined in (1).

This value enters into right-hand sides of (12) and (16) as an exponentially small factor for $X_0 \rightarrow \infty$. Though we have a very large interval of $p \in (-X_0^2, p_1)$, this factor suppresses these right-hand sides and leads to practically constant values in interval C

$$Y(p) = Y_S \equiv \lim_{r \rightarrow 0} Y(r), \quad Z(p) = Z_S \equiv \lim_{r \rightarrow 0} Z(r), \quad (33)$$

and

$$Z_S \approx Z_0, \quad Y_S \approx Y_0 Y_*, \quad (34)$$

for $M\mu \gg 1$. On account of definitions (10) of Y and (14) of Z , this means

$$r \exp\left(\frac{\alpha - \beta}{2}\right) \approx \text{const}, \quad r \frac{d\xi}{dr} \approx \text{const} \quad (35)$$

with very good accuracy for large $M\mu$. Formula (27) can be extended for $p < p_1$, i.e. to all interval C. Owing to the above estimates we get from (15) in this region (including $r \rightarrow 0$)

$$\xi(r) = -\frac{\xi_0}{\sqrt{Y_0}} \gamma(\xi_0) X_0 \ln\left(\frac{r}{r_0}\right) + \xi_0, \quad (36)$$

and from (17)

$$\chi(r) = 3 \frac{\xi_0^2}{Y_0} \gamma^2(\xi_0) X_0^2 \ln\left(\frac{r}{r_0}\right). \quad (37)$$

The metric coefficients in the Einstein frame are obtained according to (1), (10):

$$e^\alpha = \frac{Y_0}{\gamma(\xi_0)} \left(\frac{r}{r_0}\right)^{H-1}, \quad e^\beta = \frac{\gamma(\xi_0)}{Y_0} \left(\frac{r}{r_0}\right)^{H+1}, \quad (38)$$

where $H \equiv 3\xi_0^2 \gamma^2(\xi_0) X_0^2 / Y_0 \gg 1$ for $M\mu \gg 1$ and fixed ξ_0 .

Numerical tests have been carried out in case of the scalaron potential of the quadratic model (2), it satisfies conditions (20), (21), (22) for $\xi > 0$. We compared numerical calculations with previous analytic relations for $\xi_0 \sim 10^{-3} \div 10^{-5}$, $r_0 \sim (10 \div 1000)r_g$, $M\mu \sim 10^5 \div 10^{25}$. Numerical simulations confirm that approximate formulas (33),(34) in region C hold with a good accuracy for $M\mu \gtrsim 10^{11}$. Examples of dependence of limiting parameter Y_S upon $M\mu$ are shown in Fig. 1 for different sizes of the scalarization region corresponding to different values of the scalar charge. Asymptotics at large $M\mu$ are in good agreement with formula (26).

V. NUMERICAL SIMULATIONS

The results of the previous Section with fixed ξ_0 and $M\mu \rightarrow \infty$ give some idea of the structure of SSS configurations. However, the statement of the problem must be modified in case of asymptotically flat SSS systems

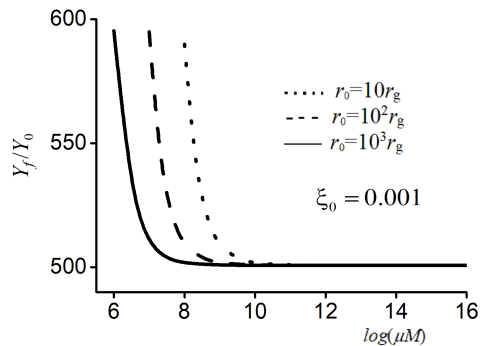


FIG. 1. The case of potential (2): dependence of limiting value Y_S/Y_0 upon $M\mu$ for three sizes r_0 of the scalarization region determined by condition $\xi(r_0) = 0.001$.

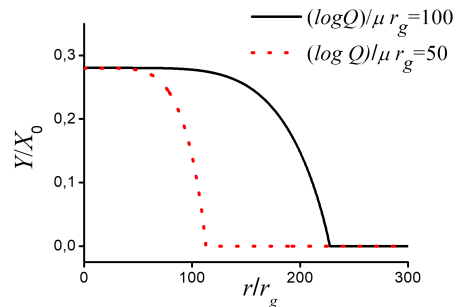


FIG. 2. The case of potential (2): $Y(r)/X_0$ against r/r_g for $\log Q = 10^{22}$ and $\log Q = 2 \cdot 10^{22}$. In this calculation we used $\mu = 10^{20}$, however the curves look almost the same for $\log(\mu) = 10 \div 20$. Corresponding sizes of the scalarization region are $113r_g$ and $228r_g$; outside this area there is an increase in $Y(r)$ that is not visible here.

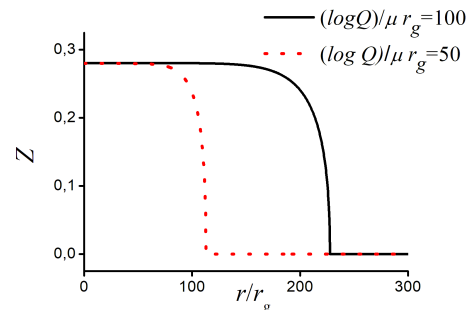


FIG. 3. The case of potential (2): $Z(r)$ against r/r_g for the same parameters as in Fig. 2. Outside the scalarization region $Z(r) > 0$ tends to zero exponentially. The curves look the same for $\log(\mu) = 10 \div 20$.

because ξ_0 , $M\mu$ and r_0 are correlated. The value ξ_0 must satisfy inequality (A8) in order that the weak-field approximation (A6) and/or (8) can be used up to $r \rightarrow r_0 + 0$. Therefore, in further numerical simulations we set the

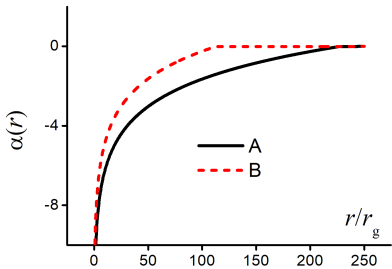


FIG. 4. The case of potential (2): $\alpha(r)$ against r/r_g . A: $\log Q = 2 \cdot 10^{22}$; B: $\log Q = 10^{22}$. The curves look the same for $\log(\mu M) = 10 \div 20$. Outside the scalarization region $\alpha(r) \approx -r_g/r$.

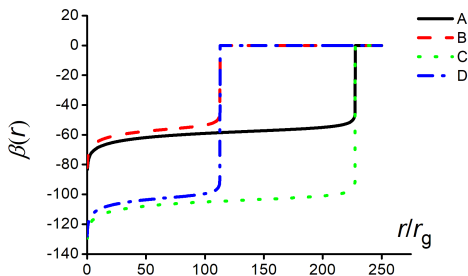


FIG. 5. The case of potential (2): $\beta(r)$ against r/r_g . A: $\mu M = 10^{20}$, $\log Q = 2 \cdot 10^{22}$; B: $\mu M = 10^{20}$, $\log Q = 10^{22}$; C: $\mu M = 10^{10}$, $\log Q = 2 \cdot 10^{22}$; D: $\mu M = 10^{10}$, $\log Q = 10^{22}$. Outside the scalarization region $\beta(r) \approx r_g/r$.

initial conditions as follows:

$$\xi(r_0) = \frac{\tilde{\xi}_0}{\sqrt{X_0}}, \quad (39)$$

where $\tilde{\xi}_0 \ll 1$. We remind that we consider the positive branch of ξ . Under condition (39) the considerations of Section IV are no longer valid and the size of the intermediate transition region B for $X_0 \rightarrow \infty$ is not small. In this case asymptotic values Y_S , Z_S (33) also exist (see Figs. 2) and 3), but relation between these values and configuration parameters M, Q must be derived numerically. The existence of limits (33) is ensured by the rapid decrease of $e^x \approx e^\beta$ as r decreases (see Figs. 4, 5). The behavior of $\xi(r)$ is shown in Fig. 6.

VI. DISCUSSION

We studied SSS configurations in the Einstein frame of the $f(R)$ gravity and found a representation of the basic equations that allowed us to derive approximate solutions and to perform numerical calculations for rather high values of $M\mu$.

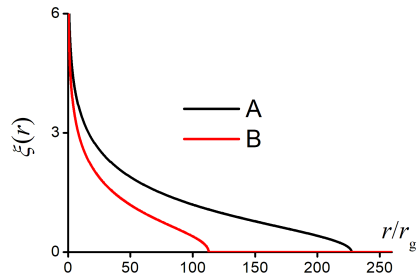


FIG. 6. The case of potential (2): $\xi(r)$ against r/r_g . A: $\mu M = 10^{20}$, $\log Q = 2 \cdot 10^{22}$; B: $\mu M = 10^{20}$, $\log Q = 10^{22}$. The curves look the same for $\log(\mu M) = 10 \div 20$. Outside the scalarization region $\xi(r)$ is given by (8).

In case of potentials satisfying conditions (20),(21), (22) that are typical for a number of known $f(R)$ gravity models, for fixed data at some $r_0 \gg r_g$, $0 < \xi_0 \ll 1$ and large enough $M\mu$, the SSS solutions exhibit similar behavior on $(0, r_0]$ that can be described analytically. The key formulas are (26), (34). Comparison with numerical simulations is shown in Fig. 1.

In case of asymptotically flat systems, there are three main regions of the radial variable with different types of behavior of the solutions.

In the region A ($r \geq r_0 \gg r_g$), we have small scalaron field that decays exponentially according to (A6). The metric takes on the Schwarzschild values.

Region B. This is an intermediate region of r with a rapid change of the metric near r_0 with subsequent (with decreasing r) smooth transition to asymptotic values (33) in the region C closer to the origin. Regions B and C are significantly different from the Schwarzschild case. In C we have practically constant values of $r d\xi/dr$ and $r \exp((\alpha - \beta)/2)$.

Our results have been obtained in the Einstein frame. The metric coefficients in the Jordan frame can be obtained by the formula (1).

Acknowledgements. I am grateful to Yu. Shtanov and O. Stashko for useful discussions. This work was partially supported by the National Research Foundation of Ukraine under project No. 2023.03/0149.

Appendix A: Approximate solutions in the region A

For $|\xi| \ll 1$ the scalaron potential and its derivative are approximated by (20) and equation (6) can be written as

$$\frac{d}{dr} \left[r^2 e^{\frac{\alpha-\beta}{2}} \frac{d\xi}{dr} \right] = \mu^2 r^2 e^{\frac{\alpha+\beta}{2}} \xi. \quad (A1)$$

For large $M\mu \gg 1$ we can apply the WKB method. Substitution of $\xi(r) = \exp[\mu u]$ into (A1) we have

$$\left(\frac{du}{dr}\right)^2 + \frac{1}{\mu} \frac{d^2u}{dr^2} + \frac{1}{\mu} \left[\frac{d}{dr} \left(2 \ln r + \frac{\alpha - \beta}{2} \right) \right] = e^\beta \quad (\text{A2})$$

Putting $u(r) = u_0(r) + \mu^{-1}u_1(r) + \dots$ in zeroth order in μ^{-1} leads to

$$\frac{du_0}{dr} = -e^{\beta/2} \quad (\text{A3})$$

where we taken into account the asymptotic behavior at the infinity. In the next order

$$u_1(r) = -\ln r - \alpha/4 + \text{Const}. \quad (\text{A4})$$

up to terms of the order of $(M\mu)^{-1}$.

Using (A3) yields

$$\frac{d\xi}{dr} = -\mu\xi e^{\beta/2} \left[1 + O\left(\frac{1}{M\mu}\right) \right]. \quad (\text{A5})$$

If $M\mu \gg 1$ and $\xi \ll 1$, in case of the Schwarzschild metric (7) we get

$$\xi(r) = \frac{Q(4/e)^{M\mu} \exp\left(-\mu r \sqrt{1 - \frac{r_g}{r}}\right)}{\left(1 - \frac{r_g}{r}\right)^{1/4} \left(1 + \sqrt{1 - \frac{r_g}{r}}\right)^{\mu r_g}} \left(\frac{r_g}{r}\right)^{1+M\mu}, \quad (\text{A6})$$

which is true up to terms of order $(M\mu)^{-1}$. This formula leads to (8) for $r \gg r_g$, However, for $M\mu \gg 1$, (A6) is effective for $r > r_g$ comparable to r_g , provided that ξ is small enough not affect the metric via (4),(5).

Now we must investigate how $\xi(r)$ affects $\alpha(r)$ and $\beta(r)$ under the conditions of the asymptotic flatness. We assume here $r \gg r_g$.

Using (7) as zeroth approximation, the first order correction to $\chi(x)$ is obtained from (4) taking into account either (8) or (A6)

$$\chi(r) = -3 \int_r^\infty dr' r' \left(\frac{d\xi}{dr}\right)^2 \approx -\frac{3}{2} \mu r \xi^2(r). \quad (\text{A7})$$

Therefore, in order that $|\chi_0| \ll 1$, one must have

$$X_0 \xi_0^2 \ll 1. \quad (\text{A8})$$

Also, under condition (A8) one can infer from (5) that $|e^{-\alpha_0}(1 - r_g/r_0) - 1| \ll 1$, $|e^{\beta_0}(1 - r_g/r_0) - 1| \ll 1$. In this case one can be sure that for $r \geq r_0$ we can use formulas (7) and (A6). In this case (A8) shows that one cannot choose $M\mu$ sufficiently large without changing ξ_0 .

-
- [1] T. P. Sotiriou and V. Faraoni, $f(R)$ theories of gravity, *Reviews of Modern Physics* **82**, 451 (2010), arXiv:0805.1726 [gr-qc].
- [2] A. De Felice and S. Tsujikawa, $f(r)$ theories, *Living Reviews in Relativity* **13**, 3 (2010), arXiv:1002.4928 [gr-qc].
- [3] S. Nojiri, S. D. Odintsov, and V. K. Oikonomou, Modified gravity theories on a nutshell: Inflation, bounce and late-time evolution, *Phys. Rept.* **692**, 1 (2017), arXiv:1705.11098 [gr-qc].
- [4] V. I. Zhdanov, O. S. Stashko, and Y. V. Shtanov, Spherically symmetric configurations in the quadratic $f(R)$ gravity, *Phys. Rev. D* **110**, 024056 (2024), arXiv:2403.16741 [gr-qc].
- [5] A. de La Cruz-Dombriz, A. Dobado, and A. L. Maroto, Black holes in $f(R)$ theories, *Phys. Rev. D* **80**, 124011 (2009), arXiv:0907.3872 [gr-qc].
- [6] S. Bhattacharya, Rotating Killing horizons in generic $F(R)$ gravity theories, *General Relativity and Gravitation* **48**, 128 (2016), arXiv:1602.04306 [gr-qc].
- [7] P. Cañate, A no-hair theorem for black holes in $f(R)$ gravity, *Classical and Quantum Gravity* **35**, 025018 (2017).
- [8] G. G. L. Nashed and S. Nojiri, Nontrivial black hole solutions in $f(R)$ gravitational theory, *Phys. Rev. D* **102**, 124022 (2020), arXiv:2012.05711 [gr-qc].
- [9] G. G. L. Nashed and S. Nojiri, Specific neutral and charged black holes in $f(R)$ gravitational theory, *Phys. Rev. D* **104**, 124054 (2021), arXiv:2103.02382 [gr-qc].
- [10] E. Hernández-Lorenzo and C. F. Steinwachs, Naked singularities in quadratic $f(R)$ gravity, *Phys. Rev. D* **101**, 124046 (2020), arXiv:2003.12109 [gr-qc].
- [11] A. A. Starobinsky, A new type of isotropic cosmological models without singularity, *Phys. Lett. B* **91**, 99 (1980).
- [12] Y. Shtanov, Light scalaron as dark matter, *Physics Letters B* **820**, 136469 (2021), arXiv:2105.02662 [hep-ph].
- [13] J. A. R. Cembranos, Dark matter from R^2 gravity, *Phys. Rev. Lett.* **102**, 141301 (2009), arXiv:0809.1653 [hep-ph].
- [14] R. A. Asanov, Static scalar and electric fields in Einstein's theory of relativity, *Soviet Journal of Experimental and Theoretical Physics* **26**, 424 (1968).
- [15] R. A. Asanov, Point source of massive scalar field in gravitational theory, *Theoretical and Mathematical Physics* **20**, 667 (1974).
- [16] D. J. Rowan and G. Stephenson, The massive scalar meson field in a Schwarzschild background space, *Journal of Physics A Mathematical General* **9**, 1261 (1976).
- [17] Y. Shtanov, V. Sahni, and S. S. Mishra, Tabletop potentials for inflation from $f(R)$ gravity, *J. Cosmol. Astroparticle Phys.* **03**, 023 (2023), arXiv:2210.01828 [gr-qc].
- [18] V. I. Zhdanov and O. S. Stashko, Static spherically symmetric configurations with N nonlinear scalar fields: Global and asymptotic properties, *Phys. Rev. D* **101**, 064064 (2020), arXiv:1912.00470 [gr-qc].